BIOCHEMISTRY
including biophysical chemistry & molecular biology

Article

pubs.acs.org/biochemistry

O_2 and Water Migration Pathways between the Solvent and Heme Pockets of Hemoglobin with Open and Closed Conformations of the Distal HisE7

Maria S. Shadrina, Gilles H. Peslherbe,* and Ann M. English*

Department of Chemistry and Biochemistry, Centre for Research in Molecular Modeling and PROTEO, Concordia University, Montreal, Quebec H4B 1R6, Canada

Supporting Information

ABSTRACT: Hemoglobin transports O_2 by binding the gas at its four hemes. Hydrogen bonding between the distal histidine (HisE7) and heme-bound O_2 significantly increases the affinity of human hemoglobin (HbA) for this ligand. HisE7 is also proposed to regulate the release of O_2 to the solvent via a transient E7 channel. To reveal the O_2 escape routes controlled by HisE7 and to evaluate its role in gating heme access, we compare simulations of O_2 diffusion from the distal heme pockets of the T and R states of HbA performed with HisE7 in its open (protonated) and closed (neutral) conformations. Irrespective of HisE7's conformation, we observe the same four or five escape routes leading directly from the α- or β-distal heme pockets to the solvent. Only 21−53% of O_2 escapes occur via these routes, with the remainder escaping through routes that encompass multiple internal cavities in HbA. The conformation of the distal HisE7 controls the escape of O_2 from the heme by altering the distal pocket architecture in a pH-dependent manner, not by gating the E7 channel. Removal of the HisE7 side chain in the GlyE7 variant exposes the distal pockets to the solvent, and the percentage of O_2 escapes to the solvent directly from the α- or β-distal pockets of the mutant increases to 70−88%. In contrast to O_2, the dominant water route from the bulk solvent is gated by HisE7 because protonation and opening of this residue dramatically increase the rate of influx of water into the empty distal heme pockets. The occupancy of the distal heme site by a water molecule, which functions as an additional nonprotein barrier to binding of the ligand to the heme, is also controlled by HisE7. Overall, analysis of gas and water diffusion routes in the subunits of HbA and its GlyE7 variant sheds light on the contribution of distal HisE7 in controlling polar and nonpolar ligand movement between the solvent and the hemes.

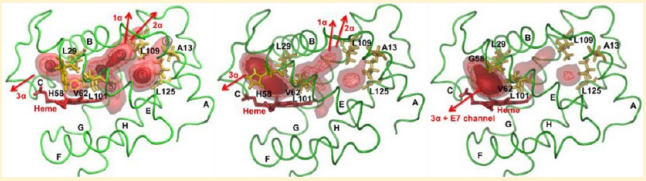

Human hemoglobin (HbA) is tasked with binding O_2 in the lungs and releasing it to tissues. The distal histidine (residue HisE7; αH58 or βH63) in its neutral $N^{\varepsilon 2}$-H tautomer donates a hydrogen bond to the heme-bound O_2, which plays a vital role in stabilizing this ligand that would otherwise be displaced by CO in the red blood cell.[1,2] Crystal structures of the HbA tetramer reveal that HisE7 also forms a visible barrier between the heme iron and solvent in the α- and β-subunits (Figure 1a,d,g),[3] which led to the hypothesis that access of the ligand to the heme is gated by swinging of the imidazole ring of HisE7 out of the distal heme pocket to form a transient ligand channel to the solvent, the alleged E7 channel.[2−5] A recent crystal structure of HbA confirmed that HisE7 can adopt an open conformation in the β-subunit (Figure 1b),[6] supporting the E7 gate hypothesis. Extension of HisE7 (H64) toward the solvent also has been reported in crystals at low pH of CO-ligated myoglobin (Mb),[7] a monomeric globin structurally related to HbA. Moreover, the pH dependence of Mb's ligand binding kinetics and the spectra of its ligated forms are attributed to protonation-linked reorientation of the imidazole ring of HisE7 and opening of the E7 channel.[4,5,8]

We observe that the neutral form of HisE7 remains in its closed conformation more than 99% of the simulated time in atomistic molecular dynamics (MD) simulations (DOI: 10.1021/acs.biochem.5b00368). This does not prevent O_2 from escaping to the solvent directly from the distal heme site with the putative E7 gate closed (DOI: 10.1021/acs.biochem.5b00368). Also, 67−77% of O_2 escapes occur from the T and R quaternary states of HbA via its interior tunnels with HisE7 closed (DOI: 10.1021/acs.biochem.5b00368). Because our simulation results with HisE7 closed are at odds with the E7 gate hypothesis, we asked if opening of HisE7 would favor direct escape to the solvent from the distal heme pockets of HbA. We found in preliminary simulations that the imidazolium ring of the protonated HisE7 spontaneously rotates out toward the solvent (Figure 1e,h) and exploit this observation here to simulate diffusion of O_2 from the distal heme pockets with HisE7 in its protonated open conformation in the high-affinity R and low-affinity T quaternary states of HbA. We additionally examine the consequences of fully removing the HisE7 side chain in the R and T states of the HbA(α,βHisE7Gly) variant, which has an open gap in its distal heme pocket (Figure 1c,f,i). Our simulations of O_2 escape provide a detailed picture of the O_2

Received: April 8, 2015
Revised: July 2, 2015
Published: July 30, 2015

DOI: 10.1021/acs.biochem.5b00369
Biochemistry 2015, 54, 5279−5289

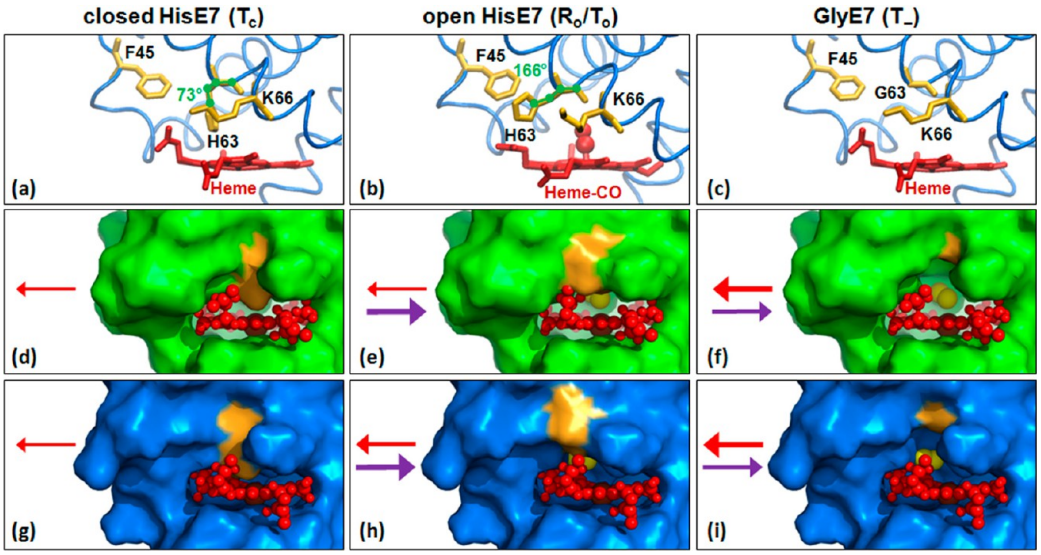

Figure 1. Distal heme pocket of T-state HbA models with a closed and open HisE7 and of the GlyE7 variant. Distal βHisE7 (βH63) side chain in (a) a closed conformation (deoxyHbA, PDB entry 2DXM),[12] (b) an open conformation (carbonmonoxyHbA, PDB entry 3D17),[6] and (c) the modeled GlyE7 variant based on PDB entry 2DXM. The backbone atoms of the β-subunit are shown as blue ribbons, and the heme is shown as red sticks. βHisE7 rotates out between residues βPheCD4 (βF45) and βLysE10 (βK66) (amber sticks) with the C−$C_α$−$C_β$−$C_γ$ torsion angle (green numbers) defining the βHisE7 conformation. (d−i) Surface models looking into the E7 channel, the shortest path between the distal site and the solvent, of the (d−f) α-distal and (g−i) β-distal heme sites of T_c, T_o, and T_. Note that O_2 (yellow ball) located in the distal site is visible looking down the E7 channel in T_o and T_ but is hidden by the closed distal HisE7 in T_c. The heme and the α- and β-subunits are represented as red spheres and green and blue surfaces, respectively. The distal E7 (αH58, αG58, βH63, or βG63) is colored amber. The thickness of the red arrow increases with the number of O_2 escapes directly from the distal heme pocket (Table 3), while the thicker purple arrow indicates that more bulk water enters the T_o vs T_ distal heme pocket. The closed HisE7 blocks the access of water to the T_c heme via the E7 channel (Figure 2).

exit routes from the distal heme sites to the solvent in each model of HbA examined but do not identify a gated gas channel. In addition to stabilizing the heme-bound O_2 ligand,[1,2] HisE7 controls its dwell time in the distal sites by modulating the architecture of the distal heme pockets.

We further probe how the protonation-linked conformation of HisE7 and its mutation to GlyE7 affect hydration of the distal heme cavity.[9] Analysis of the penetration of bulk water into HbA's subunits reveals a major role for HisE7 in gating water access and in stabilizing a distal water molecule that acts as a nonprotein barrier to binding of O_2 to the α-heme.[2,9]

COMPUTATIONAL PROCEDURES

To study O_2 escape routes in HbA, we combined all-atom Langevin dynamics simulations with $\gamma = 0.5\ ps^{-1}$ and TLES[10] as described in detail elsewhere (DOI: 10.1021/acs.biochem.5b00368).[11] In the six HbA models examined here, R_c, R_o, R_, T_c, T_o, and T_, the subscripts refer to closed (c) and open (o) conformations of HisE7 or to the absence (−) of the imidazole side chain in the GlyE7 variant. Crystal structures of deoxyHbA and CO-HbA were chosen as the initial structures for the T (PDB entry 2DXM)[12] and R (PDB entry 2DN3)[13] models, respectively, and the T_c and R_c results were obtained with the distal HisE7 in the neutral $N^{ε2}$-H tautomer,[11] which remained in the closed conformation found in the crystal structures for 99% of the MD simulation time (Figure 1a,d,g and Figure S1). T_o and R_o were modeled by HisE7 protonation in each subunit. The imidazole ring of positively charged HisE7 spontaneously rotates out toward the solvent between residues αF46 and αK61 in the α-subunit (Figure1e) and βF45 and βK66 in the β-subunit (Figure 1b,h) and remains in this conformation on the simulation time scale (Figure S1a). The initial T_ and R_ structures of the HbA(α,βHisE7Gly) variant were built from wild-type HbA by removing the HisE7 side chain (Figure 1c,f,i). The CO and distal water molecules were removed to allow placement of the O_2 copies in the distal heme sites, and after structural equilibration, all-atom MD simulations of O_2 diffusion were performed in explicit solvent at 310 K. Because the ligands do not migrate between the subunits (DOI: 10.1021/acs.biochem.5b00368),[11] 15 TLES O_2 copies were placed in the α- or β-distal site of HbA. Thirty-two replicate simulations 2 ns in duration provide 480 O_2 trajectories that separately map gas migration within each subunit for the six HbA models defined here (Table S1).

Because ligand and water molecules compete for the distal heme site,[9] water influx was examined by standard MD simulations in the absence of ligands. MD runs of 32 ns were performed to sample a large conformational subspace, including subspaces of T, R, and the T−R transition (Table S1). Notably, spontaneous quaternary change in T (DOI: 10.1021/acs.biochem.5b00368)[14] had little effect on water influx, because hydration of the distal pocket is regulated mainly by the conformation of HisE7. Fifteen independent simulations were run starting from T_c and R_c, but two simulations defined hydration of T_o, R_o, T_, and R_ because of the rapid equilibration of water between the heme pocket and solvent with the distal HisE7 open or removed. Also, we conducted four simulations for T_c and R_c with the distal heme sites occupied by a water molecule [T_{cw} and R_{cw} (Table S1)] to examine rates of escape of distal water from the α- and β-subunits.

All simulations were performed using NAMD 2.7,[15] and the simulation results were plotted using the VMD package.[16] Details of system preparation and simulation parameters were described previously in DOI: 10.1021/acs.biochem.5b00368.

DOI: 10.1021/acs.biochem.5b00369
Biochemistry 2015, 54, 5279−5289

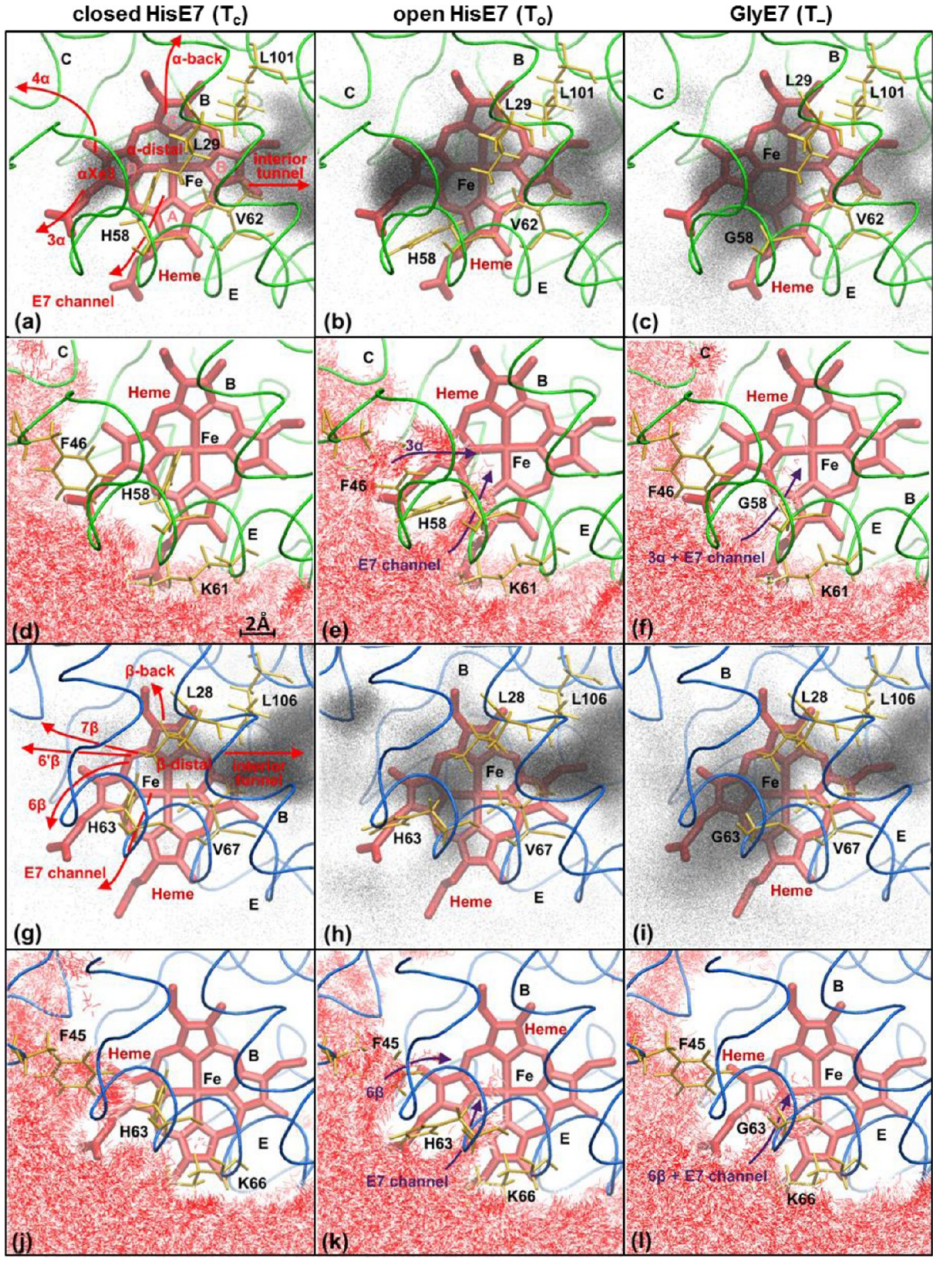

Figure 2. O_2 and water distribution around the heme of the α-subunit (green) and β-subunit (blue) of the T-state HbA models viewed from the distal side. (a–c and g–i) Black dots represent O_2 positions derived from 480 trajectories of TLES O_2 diffusion from the α- and β-distal sites labeled in panels a and g. (d–f and j–l) Red and white lines represent the water positions observed during a 0.5 ns window of ligand-free standard MD simulations (Table S1). The key distal residues that control O_2 and access of water to the heme, E7 (αH58, βH63, αG58, or βG63), PheCD4 (αF46 or βF45), and LysE10 (αK61 or βK66), as well as the B10E11G8 barrier between the heme and the interior tunnels (residues αL29, αV62, and αL101 or βL28, βV67, and βL106) are shown as amber sticks. Red arrows (panels a and g) indicate all observed O_2 escape routes from the heme distal pockets, and the frequency of portal use is summarized in Tables 1 and 2. The rotation of HisE7 toward the solvent allows extensive water access via the E7 channel and minor paths, which are marked by purple arrows in panels e and k. Analogous plots are shown for the R_c, R_o, and R_- models in Figure S4.

RESULTS

The O_2 Diffusion Tunnel Network Is Minimally Affected by Opening or Removal of the HisE7 Barrier. TLES O_2 copies placed in the α- or β-distal heme site, which corresponds to the primary geminate state on photolysis of the Fe–ligand bond,[17] exit directly to the solvent from the α- or β-distal heme site via several distal portals or diffuse through barrier B10E11G8 into the interior tunnels (Figure 2 and Figure S4). Opening or removing the HisE7 barrier does not significantly disturb the network in either subunit but does alter the O_2 distribution within the tunnels (Figures S2 and S3). Also, the quaternary state of HbA has little effect on the diffusion tunnels (Figures S2 and S3) (DOI: 10.1021/acs.biochem.5b00368). We have previously provided detailed analyses of O_2 diffusion in HbA's interior tunnels (DOI: 10.1021/acs.biochem.5b00368)[11] and concentrate here on how the protonation-linked conformations of HisE7 influence O_2 escape and access of water to the heme.

The Neutral HisE7 Very Rarely Adopts an Open Conformation during the Simulations. The open and

DOI: 10.1021/acs.biochem.5b00369
Biochemistry 2015, 54, 5279–5289

Table 1. O_2 Portal Usage in the α-Subunits of the Six HbA Models

Portal	Portal type[a]	Cavity adjacent to portal[b]	Helices & corners at portal	Residues at portal[c]	Number of O_2 escapes (based on 480 trajectories)[d]					
					T_c[f]	T_o	T_-	R_c[f]	R_o	R_-
1α	interior	αXe2	A, B, E	W14 G18 A21 T67	43	11	13	40	**15**	8
2α	interior	αXe2	B, GH	V17 Y24 H112 L113	45	26	11	11	10	1
E7 channel[e]	distal	α-distal	CE, E, heme	**H58** K61 heme	0	4	67	3	2	71
3α	distal	αXe3	CE, E, heme	F43 F46 Q54 **H58** heme	31	12		27	4	
4α	distal	αXe3	B, C, CE	E30 L34 K40 F43 L48 H50	4	2	2	18	7	11
α-back	distal	α-distal	C, G, heme	T38 T41 Y42 N97 L100	4	0	0	2	3	2
5α	interior	αXe5	E, F, heme	A65 N68 L80 L83	13	9	2	7	6	4
6α	interior	αXe6	A, GH, H	N9 A12 K16 E116 V121	21	6	3	42	30	3
Σα	**all**				**161**	**70**	**98**	**150**	**77**	**100**
Σα	**distal**				**39**	**18**	**69**	**50**	**16**	**84**

[a]Escape portals that lead to the solvent directly from the distal heme pocket are colored red and those that lead to the solvent from the interior α-tunnel black. [b]Cavities correspond to the experimental Xe docking sites in the crystal structures of HbA and HbYQ[28] and the distal site just above the heme (see Figure S2a). [c]Residues are labeled by single-letter abbreviation and numbered according to their position in the sequence. The distal αHisE7 (αH58) is bold and underlined. [d]Number of O_2 copies that escaped via each portal during 480 O_2 trajectories for each model. [e]The E7 channel (front portal) is situated between αHisE7 (αH58), αLysE10 (αK61), and heme pyrrole ring A (see Figure 2a). This is the shortest escape route to the solvent from the α-subunit. [f]Data from DOI: 10.1021/acs.biochem.5b00368.

closed conformations of the HisE7, which are defined by the $C-C_\alpha-C_\beta-C_\gamma$ torsion angle, are shown in Figure 1a,b for the β-subunit. We observe that the $N^{\varepsilon 2}$-H tautomer of HisE7 present in both T and R[1,18] can spontaneously adopt an open conformation for very short times in both subunits (Figure S1b). The most significant occurrence of the open conformation, corresponding to only ~0.7% of the simulated time, was observed in the β-subunit of R_c (Figure S1b, right panels). Because it is very rarely populated, the open conformation of the $N^{\varepsilon 2}$-H tautomer probably has little influence on O_2 diffusion in HbA. In contrast, the protonated HisE7 spontaneously rotates out toward the solvent in both the α- and β-subunits and remains in this open conformation (Figure 1e,h and Figure S1a). Similarly, protonation results in spontaneous opening of HisE7 in Mb,[19] although some[19−21] but not all simulations of Mb[22,23] find an open conformation of the neutral HisE7. This may be attributed to the use of its $N^{\delta 1}$-H tautomer, which tends to adopt the open conformation more than the $N^{\varepsilon 2}$-H tautomer,[19] and/or to insufficient sampling of protein conformation. Notably, the estimated rate of HisE7 opening and closing in HbA is 1−10 μs^{-1} at neutral pH, and the population of the open form of HisE7 was estimated to be 7%.[24] However, in this work, we strictly consider O_2 diffusion in HbA with the closed HisE7 $N^{\varepsilon 2}$-H tautomer and open protonated HisE7 to specifically compare ligand diffusion with HisE7 open and closed.

The E7 Channel Is a Minor O_2 Escape Route from the Distal Heme Pockets Even with HisE7 in Its Open Conformation. The shortest escape route to the solvent from the α- or β-subunit is between HisE7, LysE10 (αK61 or βK66), and the heme pyrrole ring A. We label this front portal the E7 channel (Figure 2a,g and Figure S4a,g) as it corresponds to the HisE7-gated channel described for Mb.[19,25,26] The long side chain of LysE10 (vs ThrE10 in Mb) together with the closed neutral HisE7 appears to effectively block the E7 channel in HbA. Nonetheless, a few ligands take advantage of a slight displacement in HisE7 to squeeze between this residue and ValE11 into a small space above heme pyrrole ring A and escape to the solvent between HisE7 and LysE10 (Figure 2a,g and Figure S4a,g). Rotation of HisE7 toward the solvent relieves the steric hindrance in the distal site, and more ligands diffuse to the protein surface (Figure 2b,h and Figure S4b,h). As a result, 8% of O_2 escapes from the HbA tetramer occur through the E7 channel upon opening of HisE7 [T_o plus R_o (Tables 1 and 2)] versus 2% with HisE7 closed [T_c and R_c (Tables 1 and 2)]. O_2 also escapes from the tetramer in the opposite direction to the E7 channel, which we label the back portal (Figure 2a,g, Figure S4a,g, and Tables 1 and 2). However, this portal is located at the $\alpha 1\beta 2$ interface and is hindered by a neighboring $\alpha 1$ or $\beta 2$ subunit, so its overall contribution to escape is low [3% in T_c and R_c and 2% in T_o and R_o (Tables 1 and 2)]. In summary, our simulations indicate that the E7 channel is a minor O_2 escape route whether E7 is opened or closed. Notably, diffusion through the closed E7 channel is also reported for Mb.[19,27]

Expansion of the Distal Heme Pockets upon HisE7 Opening Impacts Ligand Population and Escape. Ligands that diffuse from the α-distal heme site to the αXe3 cavity escape between αHisE7 and the αCE loop (portal 3α) or between this loop and α-helix B (portal 4α) (Figure 2a and Figure S4a). However, swinging of the side chain of αHisE7 out toward the solvent converts the α-distal and αXe3 sites into a

DOI: 10.1021/acs.biochem.5b00369
Biochemistry 2015, 54, 5279−5289

Table 2. O_2 Portal Usage in the β-Subunits of the Six HbA Models

Portal	Portal Type [a]	Cavity adjacent to portal [b]	Helices & corners at portal	Residues at portal [c]	Number of O_2 escapes (based on 480 trajectories) [d,f]					
					T_c [g]	T_o	T_-	R_c [g]	R_o	R_-
1β	interior	βXe1	G, H	R104 G107 N108 V134 A135 A138	91	73	23	31	35	19
2β	interior	βXe1	NA, A, E	K8 T12 W15 L75 L78	13	5	6	10	11	7
3β	interior	βXe1	NA, EF, H	V1 L81 G136	7	6	4	8	5	3
4β	interior	βXe2	AB, G	V18 E22 H117 F118	5	6	6	7	7	1
5β	interior	βXe2	AB, E	W15 V18 V20	3	4	2	4	5	6
E7 channel [e]	distal	β-distal	CD, E, heme	H63 K66 heme	5	22	242	1	12	265
6β	distal	β-distal	CD, E, heme	F42 F45 H63 heme	17	59		13	50	
6′β	distal	αXe3	CD, D, E	G46 D47 A53 N57	2	4		1	1	
7β	distal	αXe3	B, D, E	G25 M55 N57 K61	2	9	3	3	5	7
β-back	distal	β-distal	C, G, heme	F41 W37 T38 N102 L105	6	5	3	4	2	0
8β	interior	βXe1	E, F, heme	A70 F85 L88 heme	0	2	0	3	0	0
Σβ	all				151	195	289	85	133	308
Σβ	distal				32	99	248	22	70	272

[a]Escape portals that lead to the solvent directly from the distal heme pocket are colored red and those that lead to the solvent from the interior α-tunnel black. [b]Cavities correspond to the experimental Xe docking sites in the crystal structures of HbA and HbYQ[28] and the distal site just above the heme (see Figure S3a). [c]Residues are labeled by single-letter abbreviation and numbered according to their position in the sequence. The distal βHisE7 (βH63) is bold and underlined. [d]Number of O_2 copies that escaped via each portal during 480 O_2 trajectories for each model. [e]The E7 channel (front portal) is situated between βHisE7 (βH63), βLysE10 (βK66), and heme pyrrole ring A (see Figure 2g). This is the shortest escape route to the solvent from the β-subunit. [f]Many O_2 molecules entered HbA's central water-filled cavity from the β-subunit via portal 1β and immediately returned to the same β-tunnel.[11] Only those O_2 molecules that escaped to the bulk solvent during the 2 ns simulations are included in this table. [g]Data from DOI: 10.1021/acs.biochem.5b00368.

single large cavity (Figure 2b and Figure S4b). This increases the ligand dwell time in the α-distal heme pocket (Figure S2b,e vs Figure S2a,d), and the escape percent from αXe3 decreases to 17% in T_o and R_o from 26% in T_c and R_c (Table 1). Although the conformation of αHisE7 controls the time spent by the ligands in the α-heme pocket, it has little impact on the actual gas route as exemplified by representative trajectories. A single O_2 molecule placed in the α-distal site of T_o or T_c escapes to the solvent via distal portal 3α (Figure 3b vs Figure 3a) irrespective of the presence (T_c) or absence (T_o) of the αHisE7 barrier.

A docking site equivalent to αXe3 is absent from the smaller β-heme pocket (Figure 2g vs Figure 2a and Figure S4g vs Figure S4a). Thus, opening of βHisE7 increases the level of direct O_2 escape via portal 6β [located between βHisE7, βF42, and heme pyrrole D (Figure 3d,e)] to 33% in T_o and R_o from 13% in T_c and R_c (Table 2). Prompt O_2 escape from the small T_o β-distal site contrasts the relatively long ligand dwell time in the expanded T_o α-distal site (Figure 3b,e), which leads to a dramatically higher level of direct escape from the distal heme pocket in the β-subunit versus α-subunit (Table 3). Infrequently, ligands diffuse further from the β-heme to escape via portals 6′β and 7β that bracket the βCD loop (Figure 2g), with 3 and 6% of escapes occurring via these combined portals in the closed and open β-subunits, respectively (Table 2).

The HisE7Gly Mutation Dramatically Increases the Rate of Direct Escape of O_2 from the Distal Heme Pockets. Substituting the side chain of HisE7 with a hydrogen atom widens the constriction between the distal heme cavity and the solvent (Figures 1f,i and 2c,i and Figure S4c,i). O_2 molecules placed in the distal sites of the GlyE7 variant appear at the interface between the hydrophobic protein environment and the hydrophilic solvent. Thus, in T_- and R_-, close to 68−86% of escapes occur directly to the solvent through the gap formed in the wall of the α- and β-distal heme pockets, respectively (Table 2). Nevertheless, the striking >3-fold lower number of O_2 copies that escape from the α-distal versus β-distal heme pocket (Table 3) arises because the αXe3 cavity also accommodates apolar ligands in the GlyE7 variant (Figure 3c vs Figure 3f).

Water Readily Enters the Distal Heme Pockets via the Open E7 Channel and Is Gated by HisE7. HisE7 in its closed conformation together with residues LysE10 and PheCD4 (αF46 or βF45) forms a barrier that blocks the access of water to the distal sites of T_c and R_c (Figure 2d,j and Figure S4d,j). HisE7 protonation opens the E7 channel for bulk

DOI: 10.1021/acs.biochem.5b00369
Biochemistry 2015, 54, 5279−5289

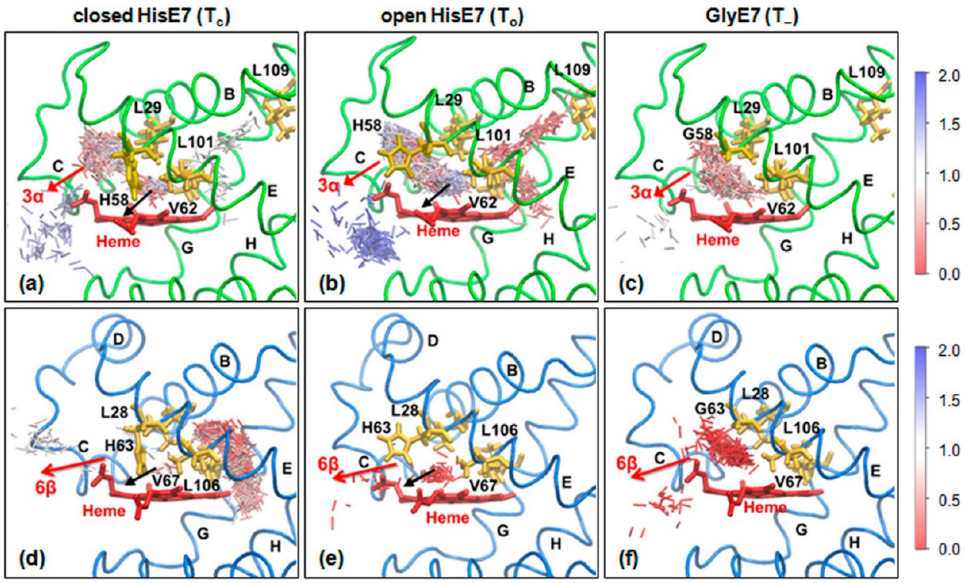

Figure 3. Escape route of a single O_2 molecule from the distal heme site to the solvent via the major distal portal in each subunit. The heat map indicates the positions of the O_2 molecule (sticks) vs simulated time (nanoseconds) that define a representative trajectory from (a–c) the α-distal heme site via portal 3α and (d–f) the β-distal heme site via portal 6β of the T_c, T_o, and T_- models. Note that the O_2 molecule escapes significantly faster from the β-distal site (d–f) than from the α-distal site (a–c). In fact, the O_2 molecule spends most of the simulated time in the β-tunnel of T_c (d) before escaping to the solvent via portal 6β, whereas opening (T_o, panel e) or removal of βHisE7 (T_-, panel f) facilitates direct escape to the solvent without β-tunnel visitation as in the trajectories selected here. Also note that in T_- the E7 channel (marked as a black arrow in panels a, b, d, and e) collapses into one exit with portal 3α (Table 1) and portals 6β and 6β' (Table 2) in the α- and β-subunits, respectively. The protein representation is described in the legend of Figure 2, and the number of O_2 escapes via portals 3α and 6β is listed in Tables 1 and 2.

Table 3. Numbers and Percentages of Direct O_2 Escapes from the Distal Heme Pockets in 480 O_2 Trajectories

model[a]	T_c[b]	T_o	T_-	R_c	R_o	R_-
α-subunit	39 (24%)	18 (26%)	69 (70%)	50 (33%)	16 (21%)	84 (84%)
β-subunit	32 (21%)	99 (51%)	248 (86%)	22 (26%)	70 (53%)	272 (88%)
average[c]	36 (22%)	58 (38%)	158 (78%)	36 (30%)	43 (37%)	178 (86%)

[a]The HbA models include the tense (T) and relaxed (R) quaternary structures with the distal HisE7 in its closed (T_c and R_c) and open (T_o and R_o) conformations or absent from the GlyE7 variant (T_- and R_-) (see the text). [b]For each model, the escape number is the number of O_2 molecules that exited to the solvent directly from the distal heme pocket of the specified subunit during 480 trajectories 2 ns in duration. The escape percent (in parentheses) is the number of molecules that exited from the distal heme pocket relative to the total number of molecules that exited the specified subunit during the 480 trajectories. See Tables 1 and 2 for a full list of O_2 escapes. [c]Average of the α- and β-subunit values for the specified model.

water to freely access the hemes via this direct route as well as via minor portals, 3α (Figure 2e and Figure S4e) and 6β (Figure 2k and Figure S4k). The expanded α-distal pocket formed upon fusion of the α-distal and αXe3 sites can simultaneously attract up to six water molecules (Figure 4b), and up to three waters are accommodated in the smaller β-distal pocket (Figure 4e). The HisE7Gly mutation exposes the distal pockets to the bulk solvent but renders them less hydrophilic (Figure 2f,l and Figure S4f,l) such that they maximally attract three water molecules (Figure 4c,f).

Water Also Enters the Distal Heme Pockets by Minor Routes. Although the access of water to the heme is strongly gated by HisE7, a number of molecules succeed in reaching the heme via routes that are not controlled by this residue. Specifically, during the 30 standard MD simulations with αHisE7 closed, four water molecules reach the αFe via the α-back, 3α, and 4α portals of T_c and R_c. Notably, during one simulation, the highly flexible αCE loop (DOI: 10.1021/acs.biochem.5b00368) undergoes a large conformational change that significantly disturbs the protein structure around the αXe3 cavity. Rotation of αPheCD4 (αF46) toward the solvent partially exposes the α-distal heme pocket, which becomes flooded with eight water molecules (Figure 4a). Figure 5a maps the trajectory of one such water molecule that enters the αXe3 cavity through the expanded 3α portal and diffuses to the α-heme. When the αCE loop returns to conformations close to that found in the crystal structure with αF46 in its closed conformation, all water molecules exit the α-distal heme pocket. Thus, a reversible conformational change in the αCE loop allows transient bulk water access to the α-heme while αHisE7 remains closed.

The highly flexible βCD loop (DOI: 10.1021/acs.biochem.5b00368) also undergoes a large conformational change with rotation of βPheCD4 (βF45) toward the solvent, allowing a water molecule to enter the smaller β-distal site through portal 6β (Figure 4d). Thus, in both subunits, bulk water can transiently access the heme with HisE7 in its closed conformation. Additionally, nine water molecules entered the β-subunit via portal 1β and reached the β-distal heme pocket with βHisE7 closed (T_c and R_c). Their path to the β-heme encompasses the experimental βXe1, βXe1′, and βXe2 cavities[28] and represents a major route for O_2 entry and escape in the β-subunit (DOI: 10.1021/acs.biochem.5b00368).[11,29] Tracking one such water in T_c (Figure 5b), we find that once in

DOI: 10.1021/acs.biochem.5b00369
Biochemistry 2015, 54, 5279–5289

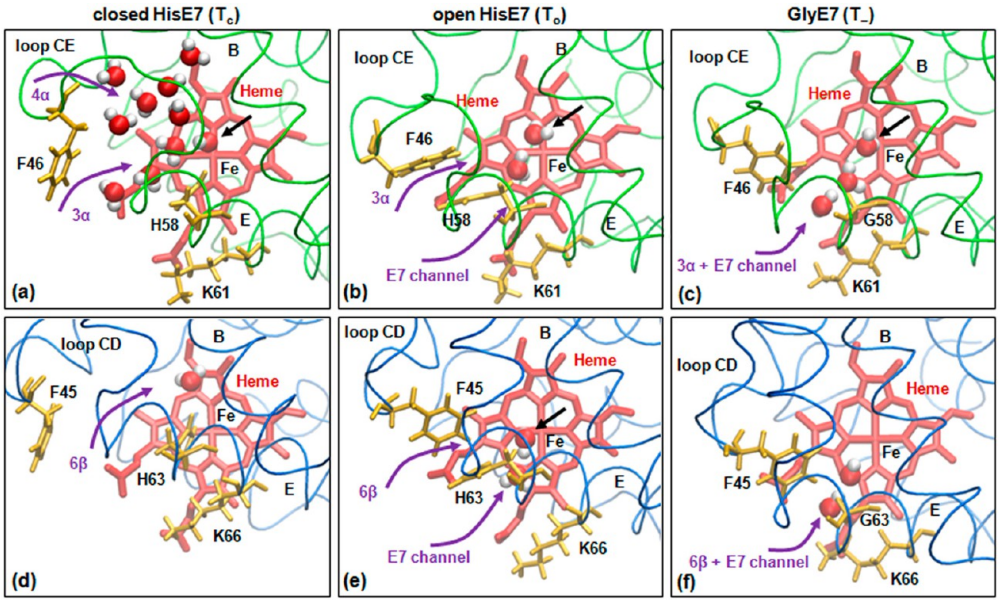

Figure 4. Figure 4. Snapshots of hydration of the distal heme pockets during the ligand-free 32-ns standard MD simulations. Representative frames show bulk water molecules that transiently access the α- and β-distal heme pockets with PheCD4 (αF46, βF45) (a and d) extended out toward the solvent in the T_c models where HisE7 is closed; and with PheCD4 in conformations similar to those in the crystal structures in the (b and e) T_o and (c and f) T_- models where HisE7 is open and removed, respectively. The protein representation is described in the legend of Figure 2, waters located within the distal pockets are represented as red (oxygen) and white (hydrogen) spheres, and external waters are omitted for clarity. The black arrow in panels a–c and e locates a water within 4.5 Å of the heme Fe (Table 4) and the purple arrows identify water access routes to the distal pockets. The open E7 channel is the major water access route but rotation of αPheCD4 transiently opens up portal 4α in panel a. However, the distal pockets in the T_c models contain no waters during most of the simulated time whereas 3–6 waters can simultaneously accumulate in the T_o and T_- models (see text for details).

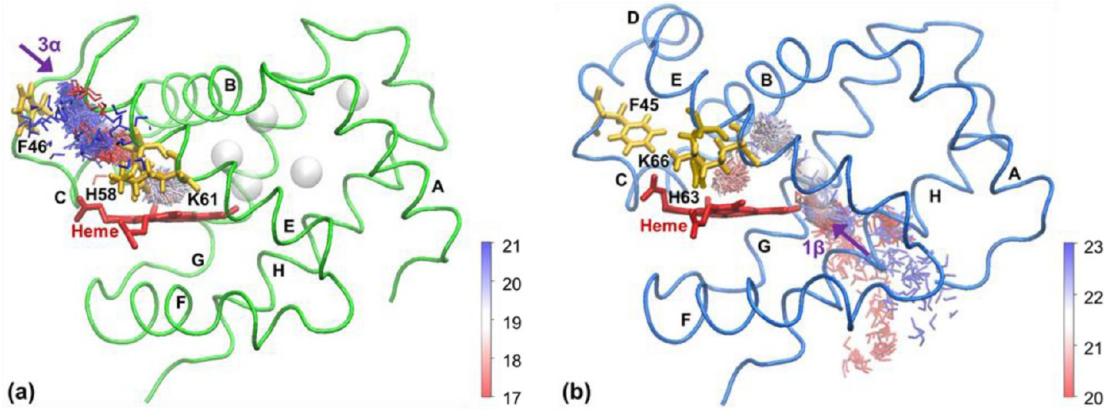

Figure 5. Entry route of a single water molecule from the bulk solvent into the distal heme sites via minor water portals 3α and 1β with HisE7 closed. A representative water trajectory from the bulk solvent to the distal heme site via (a) portal 3α (purple arrow) of the R_c α-subunit and (b) portal 1β (purple arrow) of the T_c β-subunit. Residue PheCD4 (F46) is rotated out toward the solvent allowing the entry of bulk water into the closed α-heme pocket in panel a. Heat maps indicate the position vs simulated time (nanoseconds) of the water molecule (sticks) within the subunits during the 32 ns standard MD simulations (Table S1). The protein representation is described in the legend of Figure 2, and the experimental Xe docking sites in the crystal structures of HbA and HbYQ[28] are shown as transparent white spheres.

the β-tunnel, it resides in the βXe1 cavity, which is normally occupied by a water molecule in HbA crystals,[13] and forms hydrogen bonds with the backbone carbonyls of residues βF103 and βV134. Next, the water jumps to the βXe2 site and forms hydrogen bonds to the carbonyls of residues βG24 and βG64 before crossing barrier βB10E11G8 into the β-distal heme site, where it accepts a hydrogen bond from the $N^{\varepsilon 2}$-H tautomer of βHisE7. Very rarely [~0.7% of the total simulated time (Figure S1b)], the neutral βHisE7 of R_c swings out, allowing the entry of bulk water into the β-distal pocket by the βE7 channel.

In contrast to the case in T_c and R_c, recent MD simulations reveal that water can access the distal heme pocket through the closed E7 channel in metMb.[27] Presumably, the smaller ThrE10 residue in Mb blocks the E7 channel less effectively than LysE10 in HbA and allows water exchange with HisE7 closed.[19,27] Interestingly, in the HbA(βLysE10Thr) variant (Hb Chico),[30] as in Mb,[31] a water molecule is stabilized in the E7 path to the distal heme site by interaction with HisE7 and ThrE10.

The Distal Water Occupancy, n_w, Reflects the Relative Size and Hydrophobicity of the Distal Pockets. We

DOI: 10.1021/acs.biochem.5b00369
Biochemistry 2015, 54, 5279–5289

examined the fraction of the simulated time that a water molecule lies within 4.5 Å of the Fe and found n_w values close to 0 for both subunits of T_c and R_c. Because the closed HisE7 efficiently impedes the access of bulk water to the heme, we performed additional simulations starting with a single water molecule placed in each distal site [T_{cw} and R_{cw} (Table S1)] and observed that on average the water remained in the α-site for 12.5 ns and in the β-site for 2 ns. Once this water escaped to the bulk solvent, it was not replaced during the remainder of the 32 ns simulation. In fact, on the basis of the number of observed entry events divided by the total standard MD simulation time (Table S1), we estimate average rates of 2 and 5 μs^{-1} for the entry of water from the solvent into the empty α- and β-distal heme sites, respectively, of T_c or R_c. From these rates and the average dwell times of 12.5 and 2 ns, n_w values close to 0 are expected for both closed subunits [T_c and R_c (Table 4)] as seen in the simulations starting from the empty closed distal sites. In contrast, bulk water rapidly enters the open E7 channel and a distal water is observed for much of the simulated time in T_o (Figure 4b,e) and R_o (data not shown). As for O_2 occupancy (Figure 3b,e), the larger α-distal site better accommodates the water molecule than the β-site (Figure 4) and the average simulated n_w values are 0.56 and 0.29, respectively [T_o and R_o (Table 4)]. Also, despite the access of bulk water to the T_ and R_ hemes, small simulated n_w values reveal the lower hydrophobicity of the distal heme sites in the HisE7Gly variant [T_ and R_ (Table 4)].

Table 4. Water Occupancies (n_w) of the Distal Heme Sites of HbA

HbA model	$n_{w\ calcd}$, α-subunit[a]	$n_{w\ calcd}$, β-subunit[a]	HbA state	$n_{w\ exp}$, α-subunit	$n_{w\ exp}$, β-subunit
T_c, R_c[b]	0.01	0.003	T_c (crystal)[c]	1	0
T_o, R_o[b]	0.56	0.29	T_o[d]	<1	>0
T_, R_[b]	0.10	0.07	T_[e]	<1	>0
isolated subunit	ND	ND	isolated subunit (solution)[f]	0.64	0.23

[a]The n_w values estimated from the simulations correspond to the fractions of the simulated time that a water molecule is found within 4.5 Å of the heme Fe. Note that the T and R n_w values are not distinguishable because of the variability in the simulations. ND means not determined. [b]The HbA models include the tense (T) and relaxed (R) quaternary structures with the distal HisE7 in its closed (T_c and R_c) or open (T_o and R_o) conformation or absent from the GlyE7 variant (T_ and R_) (see the text). [c]n_w values from the room-temperature, high-resolution crystal structure of the deoxyHb tetramer with the distal HisE7 in its closed conformation in both the α- and β-subunits.[13] Note that the distal water is 3.3−3.5 Å from the heme Fe in the α-subunit. [d]We predict a lower n_w in the α-subunit of T_o than in that of T_c because the open HisE7 is less effective than the closed HisE7 in stabilizing a distal water as seen in Mb.[43] Opening of the E7 channel allows access of water to the β-distal heme pocket (Figure 2), so n_w is likely >0. [e]We predict a lower n_w in the α-subunit of T_ than in that of T_c because the AlaE7 variant and wild-type Mb have n_w values of 0.4 and 0.84, respectively.[44] In the T_ β-subunit, n_w is assumed to be >0 because of the exposure of the distal heme pocket. [f]Experimental n_w values from spectrokinetic analysis of the photolyzed isolated HbA subunits.[9]

DISCUSSION

The Protonation-Linked Conformation of HisE7 Regulates the Diffusion of Gas from the Distal Heme Pockets to the Solvent by Altering the Heme Pocket Architecture.

Our simulations demonstrate that the conformation of the distal HisE7 is strongly coupled to its protonation state. In R (Figure S1) and T (data not shown), the neutral $N^{\varepsilon 2}$-H tautomer of HisE7 very rarely adopts an open conformation whereas its protonated imidazolium form spontaneously rotates out toward the solvent and remains in this open conformation essentially 100% of the simulated time. HisE7 in its closed and open conformations contributes to an H-bonding network at the water−protein interface together with LysE10, the heme propionates, and bulk water molecules. The imidazole ring of closed HisE7 H-bonds to a neighboring bulk water molecule; open HisE7 is more flexible, and its imidazole ring readily flips, switching between H-bonding to the αGlnE3 or βLysE3 carbonyl, a heme propionate, and up to two water molecules. Notably, one or two water molecules are always present between the open HisE7 and LysE10, which probably promotes the entry of bulk water into the distal site but hinders the escape of apolar gas through the open E7 channel (Figure 2, Figure S4, and Tables 1 and 2). Opening of HisE7 expands the distal heme pockets but does not create any new exit routes for O_2 (Tables 1 and 2). We observe a 3-fold increase in the ligand escape number from the open β-distal pocket, but this is offset by a 3-fold decrease in the number exiting from the open α-distal pocket (Table 3). Hence, the average escape percent directly from the open distal pockets increases only to 38% from 26% in the closed pockets (T_o and R_o values vs T_c and R_c values in Table 3). Upon removal of the HisE7 barrier and heme exposure as in the GlyE7 variant, the average escape percent from the distal pockets jumps to 82% (T_ and R_ values in Table 3), but again, >3-fold more ligands escape directly from the β-distal vs α-distal site.

Our simulations show that the comparatively small escape numbers upon opening or removal of αHisE7 (Tables 1 and 2) arise because the expanded open α-distal pocket readily attracts ligands [T_o, R_o, T_, and R_ (Figure 2b,c and Figure S2 and S4b,c). Fusing of the αXe3 and α-heme sites into a single large cavity deters direct escape to the solvent, while the absence of a site analogous to αXe3 in the β-subunit strongly increases the rate of direct escape from the smaller β-distal pocket (Figure 2h,i, Figures S3 and S4h,i, and Tables 1 and 2). Furthermore, expansion of the distal α-heme pocket also attenuates the escape of the ligands from the α-interior tunnels because the total number of escapes from the α-subunit is halved upon αHisE7 opening [$\sum\alpha$ all values (Table 1)] but significantly increased upon βHisE7 opening in the β-subunit [$\sum\beta$ all values (Table 2)]. Mutation of HisE7 to a large Trp also affects the distal pocket architecture, resulting in different ligand recombination kinetics (DOI: 10.1021/acs.biochem.5b00368).[2,24] For example, in our previous work, we showed that the indole ring in its closed conformation found in the crystal structure of the T αTrpE7 variant[24] prevents heme access for ligands from both the solvent and the α-tunnel (Figure 9a of DOI: 10.1021/acs.biochem.5b00368). In contrast, β-heme access is increased in the R βTrpE7 variant[24] (Figure 9b of DOI: 10.1021/acs.biochem.5b00368), where the indole ring is rotated outward from the distal site. Because the indole group adopts the position close to the open conformation of the native imidazole group during the simulations, the diffusion tunnels in the two models are similar (Figure 9b of DOI: 10.1021/acs.biochem.5b00368 vs Figure S3e). Moreover, 57% (Table S4 of DOI: 10.1021/acs.biochem.5b00368) and 53% (Table 2) of ligands escape from the distal pockets in the R βTrpE7 and R_o models, respectively,

DOI: 10.1021/acs.biochem.5b00369
Biochemistry 2015, 54, 5279−5289

with similar numbers of total escapes ($\sum\beta$ all values). The latter observations emphasize the role of the distal pocket architecture upon the escape of the ligands from the protein. Notably, in comparison to HisE7 opening or mutation, the quaternary state of HbA has little effect on the escape of O_2 from the distal pocket versus the interior tunnels (Table 3) or upon entry of bulk water into the distal pocket (Figure 2 vs Figure S4).

In summary, the conformation of the distal HisE7 would control the escape of O_2 from the heme by altering the distal pocket architecture in a pH-dependent manner, not by gating the E7 channel as proposed previously.[2−5] Actually, on the basis of the portal preference observed in our simulations (Tables 1 and 2), the extent of gas exchange between the heme and solvent via the open E7 channel may be considerably less than predicted.[2,24,32,33] Experimental evidence that ligands escape via routes other than the open E7 channel comes from time-resolved crystallography experiments with HbA and Mb, which reveal the release of the ligand to the solvent but not opening of HisE7.[33−35]

HisE7 Gates the Access of Bulk Water to the Distal Heme Pockets and Controls n_w, the Distal Water Occupancy. When HisE7 swings out of the distal pocket, numerous water molecules enter and exit through the E7 channel, transiently occupying the distal heme site (Figure 2e,k, Figure S4e,k, and Figure 4b,e). Our calculated distal water occupancy numbers are remarkably similar to those estimated for the isolated α-subunits (0.64) and β-subunits (0.23) from spectrokinetic measurements following heme-Fe-CO photolysis in a neutral solution (Table 4).[9] Thus, photolysis may transiently populate an open or partially open HisE7 conformation in the isolated subunits.

The simulated n_w is ∼0 for both subunits when HisE7 in closed [T_c and R_c (Table 4)]. Zero water occupancy is consistent with the absence of a water molecule in the closed β-distal site of deoxyHbA crystals at room temperature, but a noncoordinated distal water with an n_w of 1 is present at 3.3−3.5 Å from the Fe in the α-subunit [T_c crystals (Table 4)].[13] Our simulations suggest rates of entry of bulk water from the solvent into the closed, empty α- and β-distal heme sites on the order of 2 and 5 μs^{-1}, respectively, in agreement with the entry rates of 6 μs^{-1} for the isolated α- and β-subunits of HbA and 9 μs^{-1} for Mb from the spectrokinetic measurements,[9] or the ∼1 μs time scale predicted for water entry by time-resolved crystallography of photolyzed MbCO.[34] Distal water is predicted from the spectrokinetic data[9] to exit the isolated α- and β-subunits at rates of 3.4 and 20 μs^{-1}, respectively, whereas a distal water placed in the closed α- and β-distal sites of the HbA tetramer escapes at estimated rates of 12.5 and 2 ns^{-1}, respectively, during the simulations. Reasons for the discrepancy between the simulated and experimental water exit rates from the closed α-distal site, and the resultant simulated n_w of ∼0 versus an observed value of 1 in deoxyHbA crystals (Table 4), are not obvious but warrant further investigation because both simulation and experiment[2,9,29,34] demonstrate that the closed distal pockets of HbA and Mb cannot simultaneously accommodate a water and an O_2 molecule. Thus, a distal water will prevent direct diffusion of gas into the closed α-distal site, acting as a nonprotein barrier to ligand association with the α-heme.[2,9]

Lowering this water barrier is thought to contribute to the significant increase in the experimental ligand binding rates with small apolar E7 variants of HbA and Mb[2,36] that exhibit reduced levels of distal site hydration.[9,37] In agreement with experiment, n_w is 4−6-fold lower in the α- and β-distal sites of the GlyE7 variant than in the open wild-type sites [T_ and R_ vs T_o and R_o (Table 4)], which can be expected from the water distribution around their hemes (Figure 2f,l vs Figure 2e,k and Figure S4f,l vs Figure S4e,k).

The predicted rate of HisE7 opening is 1−10 μs^{-1} at neutral pH,[8,24] comparable to the rates of entry of bulk water of 2 and 5 μs^{-1} into the closed distal sites estimated from the simulations. Hence, despite the dominance of the open E7 channel as a water route between the heme and bulk solvent (Figure 2), water likely enters the closed and open distal sites with a similar frequency around pH 7.4. The highly flexible αCE and βCD loops can undergo significant conformational changes during the simulations, allowing bulk water access to the heme near PheCD4 (αF46 and βF45) with HisE7 closed (Figure 4a,d). Also, simulations reveal that diffusion through the hydrophobic tunnels may allow bulk water access (egress) to (from) the closed distal sites (Figure 5). Thus, the simulations identify a conformational change in αCE and βCD loops and diffusion through the hydrophobic interior tunnels as a means of access of water to the heme in addition to the E7 channel gated by HisE7.[2,9]

HisE7's Protonation-Linked Conformational Equilibrium May Participate in Many of HbA's Functions. The donation of a hydrogen bond from the neutral $N^{\varepsilon 2}$-H tautomer of HisE7 stabilizes the heme-bound O_2. Loss of this hydrogen bond upon protonation and rotation of HisE7 toward the solvent contributes to the well-documented enhanced release of O_2 from HbA at low pH, which serves to promote rapid tissue oxygenation.[38] Notably, opening and closing of the distal HisE7 trigger enhanced escape of free O_2 from the β- and α-subunits, respectively, of wild-type HbA [$\sum$all values (Tables 1 and 2)]. Thus, as HbA undergoes the transition from R_c to T_o, which can be triggered as red blood cells undergo the transition between the lungs and highly metabolizing tissues, escape from the β-subunit is promoted at the expense of the α-subunit. Escape from the β-subunit is also favored for both the R_ and T_ models of the GlyE7 variant, which additionally exhibits Fe−O_2 dissociation rates that are 10−40-fold faster than for wild-type HbA[2] due to the absence of a distal hydrogen bond to heme-bound O_2.

In addition to gating bulk water access to the distal sites (Figure 2 and Figure S4), the distal HisE7 most likely gates access of other physiological polar ligands, including NO_2^-. The well-studied nitrite reductase activity of deoxyHbA reduces NO_2^- to vasoactive NO to increase blood flow in highly metabolizing tissues.[39,40] The access of NO_2^- to the heme via the open E7 channel would be consistent with reports that the nitrite reductase activity of red blood cells increases upon HbA deoxygenation[41] as the intracellular pH decreases with O_2 release. Low-pH-induced opening of HisE7 will also facilitate reaction of a second molecule with a heme-bound ligand, which is not accessible in the closed distal heme sites. For example, in the well-documented reaction of free NO with oxyHbA or free O_2 with nitrosylHbA to give metHbA and NO_3^- as products,[42] HisE7 opening will both expand the distal heme pocket to allow access of the reactant to the Fe-bound ligand and promote escape of NO_3^- through the E7 channel.

■ CONCLUSIONS

Examination at the atomic level of O_2 and water migration routes in HbA sheds new light on the role of HisE7. Our

DOI: 10.1021/acs.biochem.5b00369
Biochemistry 2015, 54, 5279−5289

simulations reveal that HisE7 regulates O_2 escape by controlling how well this apolar ligand is accommodated in the distal pockets and not by gating its exit. Protonation-linked interconversion between open and closed conformations of HisE7 alters the volume and hydration of the heme pocket in each subunit, which critically determines how much time O_2 spends in the distal sites. This is clearly demonstrated by the 3-fold decrease in direct O_2 escapes from the expanded α-pocket versus the 3-fold increase in direct escapes from the β-pocket when HisE7 is switched from its closed to open conformation in both the R and T states. The open E7 channel is the major entry−exit route for water and most probably other polar molecules such as NO_2^- and NO_3^-. Passage of polar molecules through the E7 channel is gated by HisE7, and its protonation and opening allow these molecules access to the heme, in addition to providing a reactant access to a heme-bound ligand.

■ ASSOCIATED CONTENT

Supporting Information

The Supporting Information is available free of charge on the ACS Publications website at DOI: 10.1021/acs.biochem.5b00369.

Figures showing maps of O_2 population within the kinetically accessible diffusion tunnels of T_c, T_o, T_-, R_c, R_o, and R_- and of water and O_2 distributions around the heme in R_c, R_o, and R_-, plots of the HisE7 torsion angle versus simulation time for R_c and R_o, and tables summarizing the simulations performed (PDF)

■ AUTHOR INFORMATION

Corresponding Authors

*E-mail: gilles.peslherbe@concordia.ca. Telephone: 514-848-2424-3335. Fax: 514-848-2864.

*E-mail: ann.english@concordia.ca. Telephone: 514-848-2424-3338. Fax: 514-848-2864.

Funding

This work was funded by FRQ-NT (Quebec) and NSERC (Canada). M.S.S. is the recipient of a PROTEO postdoctoral fellowship (FRQ-NT), and G.H.P. is a Concordia University Research Fellow.

Notes

The authors declare no competing financial interest.

■ ACKNOWLEDGMENTS

Computational resources were provided by Calcul Québec, Compute Canada and the Centre for Research in Molecular Modeling (CERMM).

■ ABBREVIATIONS

HbA, human hemoglobin; R, relaxed quaternary state; T, tense quaternary state; Mb, myoglobin; MD, molecular dynamics; PDB, Protein Data Bank; TLES, temperature-controlled locally enhanced sampling.

■ REFERENCES

(1) Lukin, J. A., Simplaceanu, V., Zou, M., Ho, N. T., and Ho, C. (2000) NMR reveals hydrogen bonds between oxygen and distal histidines in oxyhemoglobin. *Proc. Natl. Acad. Sci. U. S. A. 97*, 10354−10358.

(2) Birukou, I., Schweers, R. L., and Olson, J. S. (2010) Distal histidine stabilizes bound O_2 and acts as a gate for ligand entry in both subunits of adult human hemoglobin. *J. Biol. Chem. 285*, 8840−8854.

(3) Perutz, M. F., and Mathews, F. S. (1966) An x-ray study of azide methaemoglobin. *J. Mol. Biol. 21*, 199−202.

(4) Tian, W. D., Sage, J. T., and Champion, P. M. (1993) Investigations of ligand association and dissociation rates in the "open" and "closed" states of myoglobin. *J. Mol. Biol. 233*, 155−166.

(5) Zhu, L., Sage, J. T., Rigos, A. A., Morikis, D., and Champion, P. M. (1992) Conformational interconversion in protein crystals. *J. Mol. Biol. 224*, 207−215.

(6) Jenkins, J. D., Musayev, F. N., Danso-Danquah, R., Abraham, D. J., and Safo, M. K. (2009) Structure of relaxed-state human hemoglobin: insight into ligand uptake, transport and release. *Acta Crystallogr., Sect. D: Biol. Crystallogr. 65*, 41−48.

(7) Yang, F., and Phillips, G. N., Jr. (1996) Crystal structures of CO-, deoxy- and met-myoglobins at various pH values. *J. Mol. Biol. 256*, 762−774.

(8) Tian, W. D., Sage, J. T., Champion, P. M., Chien, E., and Sligar, S. G. (1996) Probing heme protein conformational equilibration rates with kinetic selection. *Biochemistry 35*, 3487−3502.

(9) Esquerra, R. M., Lopez-Pena, I., Tipgunlakant, P., Birukou, I., Nguyen, R. L., Soman, J., Olson, J. S., Kliger, D. S., and Goldbeck, R. A. (2010) Kinetic spectroscopy of heme hydration and ligand binding in myoglobin and isolated hemoglobin chains: an optical window into heme pocket water dynamics. *Phys. Chem. Chem. Phys. 12*, 10270−10278.

(10) Cohen, J., Kim, K., King, P., Seibert, M., and Schulten, K. (2005) Finding gas diffusion pathways in proteins: application to O_2 and H_2 transport in CpI [FeFe]-hydrogenase and the role of packing defects. *Structure 13*, 1321−1329.

(11) Shadrina, M. S., English, A. M., and Peslherbe, G. H. (2012) Effective Simulations of Gas Diffusion Through Kinetically Accessible Tunnels in Multisubunit Proteins: O_2 Pathways and Escape Routes in T-state Deoxyhemoglobin. *J. Am. Chem. Soc. 134*, 11177−11184.

(12) Chatake, T., Shibayama, N., Park, S. Y., Kurihara, K., Tamada, T., Tanaka, I., Niimura, N., Kuroki, R., and Morimoto, Y. (2007) Protonation states of buried histidine residues in human deoxy-hemoglobin revealed by neutron crystallography. *J. Am. Chem. Soc. 129*, 14840−14841.

(13) Park, S. Y., Yokoyama, T., Shibayama, N., Shiro, Y., and Tame, J. R. (2006) 1.25 A resolution crystal structures of human haemoglobin in the oxy, deoxy and carbonmonoxy forms. *J. Mol. Biol. 360*, 690−701.

(14) Hub, J. S., Kubitzki, M. B., and de Groot, B. L. (2010) Spontaneous quaternary and tertiary T-R transitions of human hemoglobin in molecular dynamics simulation. *PLoS Comput. Biol. 6*, e1000774.

(15) Phillips, J. C., Braun, R., Wang, W., Gumbart, J., Tajkhorshid, E., Villa, E., Chipot, C., Skeel, R. D., Kale, L., and Schulten, K. (2005) Scalable molecular dynamics with NAMD. *J. Comput. Chem. 26*, 1781−1802.

(16) Humphrey, W., Dalke, A., and Schulten, K. (1996) VMD: visual molecular dynamics. *J. Mol. Graphics 14*, 33−38.

(17) Adachi, S., Park, S. Y., Tame, J. R., Shiro, Y., and Shibayama, N. (2003) Direct observation of photolysis-induced tertiary structural changes in hemoglobin. *Proc. Natl. Acad. Sci. U. S. A. 100*, 7039−7044.

(18) Kovalevsky, A. Y., Chatake, T., Shibayama, N., Park, S. Y., Ishikawa, T., Mustyakimov, M., Fisher, Z., Langan, P., and Morimoto, Y. (2010) Direct determination of protonation states of histidine residues in a 2 A neutron structure of deoxy-human normal adult hemoglobin and implications for the Bohr effect. *J. Mol. Biol. 398*, 276−291.

(19) Boechi, L., Arrar, M., Marti, M. A., Olson, J. S., Roitberg, A. E., and Estrin, D. A. (2013) Hydrophobic effect drives oxygen uptake in myoglobin via histidine E7. *J. Biol. Chem. 288*, 6754−6762.

(20) Maragliano, L., Cottone, G., Ciccotti, G., and Vanden-Eijnden, E. (2010) Mapping the network of pathways of CO diffusion in myoglobin. *J. Am. Chem. Soc. 132*, 1010−1017.

(21) Bossa, C., Anselmi, M., Roccatano, D., Amadei, A., Vallone, B., Brunori, M., and Di Nola, A. (2004) Extended molecular dynamics simulation of the carbon monoxide migration in sperm whale myoglobin. *Biophys. J. 86*, 3855−3862.

DOI: 10.1021/acs.biochem.5b00369
Biochemistry 2015, 54, 5279−5289

(22) Ceccarelli, M., Anedda, R., Casu, M., and Ruggerone, P. (2008) CO escape from myoglobin with metadynamics simulations. *Proteins: Struct., Funct., Genet. 71*, 1231−1236.
(23) Cohen, J., and Schulten, K. (2007) O_2 migration pathways are not conserved across proteins of a similar fold. *Biophys. J. 93*, 3591−3600.
(24) Birukou, I., Soman, J., and Olson, J. S. (2011) Blocking the gate to ligand entry in human hemoglobin. *J. Biol. Chem. 286*, 10515−10529.
(25) Ruscio, J. Z., Kumar, D., Shukla, M., Prisant, M. G., Murali, T. M., and Onufriev, A. V. (2008) Atomic level computational identification of ligand migration pathways between solvent and binding site in myoglobin. *Proc. Natl. Acad. Sci. U. S. A. 105*, 9204−9209.
(26) Johnson, K. A., Olson, J. S., and Phillips, G. N., Jr. (1989) Structure of myoglobin-ethyl isocyanide. Histidine as a swinging door for ligand entry. *J. Mol. Biol. 207*, 459−463.
(27) Scorciapino, M. A., Robertazzi, A., Casu, M., Ruggerone, P., and Ceccarelli, M. (2010) Heme proteins: the role of solvent in the dynamics of gates and portals. *J. Am. Chem. Soc. 132*, 5156−5163.
(28) Savino, C., Miele, A. E., Draghi, F., Johnson, K. A., Sciara, G., Brunori, M., and Vallone, B. (2009) Pattern of cavities in globins: the case of human hemoglobin. *Biopolymers 91*, 1097−1107.
(29) Takayanagi, M., Kurisaki, I., and Nagaoka, M. (2013) Oxygen entry through multiple pathways in T-state human hemoglobin. *J. Phys. Chem. B 117*, 6082−6091.
(30) Bonaventura, C., Cashon, R., Bonaventura, J., Perutz, M., Fermi, G., and Shih, D. T. (1991) Involvement of the distal histidine in the low affinity exhibited by Hb Chico (Lys beta 66——Thr) and its isolated beta chains. *J. Biol. Chem. 266*, 23033−23040.
(31) Cheng, X. D., and Schoenborn, B. P. (1991) Neutron diffraction study of carbonmonoxymyoglobin. *J. Mol. Biol. 220*, 381−399.
(32) Birukou, I., Maillett, D. H., Birukova, A., and Olson, J. S. (2011) Modulating distal cavities in the alpha and beta subunits of human HbA reveals the primary ligand migration pathway. *Biochemistry 50*, 7361−7374.
(33) Schotte, F., Cho, H. S., Soman, J., Wulff, M., Olson, J. S., and Anfinrud, P. A. (2013) Real-time tracking of CO migration and binding in the alpha and beta subunits of human hemoglobin via 150-ps time-resolved Laue crystallography. *Chem. Phys. 422*, 98−106.
(34) Schotte, F., Soman, J., Olson, J. S., Wulff, M., and Anfinrud, P. A. (2004) Picosecond time-resolved X-ray crystallography: probing protein function in real time. *J. Struct. Biol. 147*, 235−246.
(35) Tomita, A., Kreutzer, U., Adachi, S., Koshihara, S. Y., and Jue, T. (2010) 'It's hollow': the function of pores within myoglobin. *J. Exp. Biol. 213*, 2748−2754.
(36) Scott, E. E., Gibson, Q. H., and Olson, J. S. (2001) Mapping the pathways for O_2 entry into and exit from myoglobin. *J. Biol. Chem. 276*, 5177−5188.
(37) Quillin, M. L., Arduini, R. M., Olson, J. S., and Phillips, G. N., Jr. (1993) High-resolution crystal structures of distal histidine mutants of sperm whale myoglobin. *J. Mol. Biol. 234*, 140−155.
(38) Johnson, D. E., and Casey, J. R. (2011) Cytosolic H+ microdomain developed around AE1 during AE1-mediated Cl^-/HCO_3^- exchange. *J. Physiol. 589*, 1551−1569.
(39) Singel, D. J., and Stamler, J. S. (2005) Chemical physiology of blood flow regulation by red blood cells: the role of nitric oxide and S-nitrosohemoglobin. *Annu. Rev. Physiol. 67*, 99−145.
(40) Laterreur, J., and English, A. M. (2007) Hemoglobin S-nitrosation on oxygenation of nitrite/deoxyhemoglobin incubations is attenuated by methemoglobin. *J. Inorg. Biochem. 101*, 1827−1835.
(41) Huang, Z., Shiva, S., Kim-Shapiro, D. B., Patel, R. P., Ringwood, L. A., Irby, C. E., Huang, K. T., Ho, C., Hogg, N., Schechter, A. N., and Gladwin, M. T. (2005) Enzymatic function of hemoglobin as a nitrite reductase that produces NO under allosteric control. *J. Clin. Invest. 115*, 2099−2107.
(42) Herold, S., and Rock, G. (2005) Mechanistic studies of the oxygen-mediated oxidation of nitrosylhemoglobin. *Biochemistry 44*, 6223−6231.
(43) Esquerra, R. M., Jensen, R. A., Bhaskaran, S., Pillsbury, M. L., Mendoza, J. L., Lintner, B. W., Kliger, D. S., and Goldbeck, R. A. (2008) The pH dependence of heme pocket hydration and ligand rebinding kinetics in photodissociated carbonmonoxymyoglobin. *J. Biol. Chem. 283*, 14165−14175.
(44) Goldbeck, R. A., Bhaskaran, S., Ortega, C., Mendoza, J. L., Olson, J. S., Soman, J., Kliger, D. S., and Esquerra, R. M. (2006) Water and ligand entry in myoglobin: assessing the speed and extent of heme pocket hydration after CO photodissociation. *Proc. Natl. Acad. Sci. U. S. A. 103*, 1254−1259.

DOI: 10.1021/acs.biochem.5b00369
Biochemistry 2015, 54, 5279−5289